

## Combination of Active and Passive Microwave to Estimate Snowpack Properties in Great Lakes Area

AMIR E. AZAR<sup>1</sup>, TARENDRA LAKHANKAR<sup>1</sup>,  
NARGES SHAHROUDI<sup>1</sup>, AND REZA KHANBILVARDI<sup>1</sup>

### ABSTRACT

In this research we examine active and passive microwave to snow water equivalent (SWE) and to investigate the potential of combining active and passive microwaves to improve the estimation of SWE. The study area is located in Great Lakes area between the latitudes of 41N–49N and the longitudes of 87W–98W. Passive microwave are obtained from DMSP SSM/I sensors provided by NSIDC. Active microwave were obtained from different sensors: 1) RADARSAT C-Band SAR. 2) QuikSCAT Ku-band (13.4GHz) for both vertical and horizontal polarizations. The ground truth data was obtained from SNODAS data set produced by NOHRSC. An Artificial Neural Network model was defined to model various combinations of inputs to SWE. The results indicate that none of the active microwave channels produce satisfactory results. However, when combined with passive microwave, they improve the estimated SWE.

### INTRODUCTION

Microwave remote sensing techniques have been effective for monitoring snowpack parameters (snow extend, depth, water equivalent, wet/dry state). Snow parameters are extremely important for input to hydrological models for understanding changes in climate due to global warming. Snow parameters been investigated by numerous researchers using many sensors such as SMMR and SSMI for passive microwave and SAR and QSCAT for active microwave. Space-borne microwave sensors can monitor characteristics of seasonal snow cover at high latitudes regardless of lighting conditions, time of the day, and vegetation.

In passive microwave radiometer, microwave energy emitted from the ground surface is transmitted through the snow layer into the atmosphere and recorded by the sensor. Snow parameters can be extracted from remote sensing data by empirical algorithms. Hallikainen (1984) introduced his algorithm for estimating SWE using passive microwave SMMR data. The process involved the subtraction vertical polarizations of 18 and 37 GHz frequencies. The subtracted value, dT, was used to define linear relationships between dT and SWE. Chang et al. (1987) proposed using the difference between the horizontally polarized channels SMMR 37 GHz and 18 GHz to derive snow depth – brightness temperature relationship for a uniform snow field (Chang et al 1987). Goodison and Walker (1995) introduced the most widely used algorithm for North America. The algorithm was originally for Canadian prairies. It defines a linear relationship between GTV  $([37V-19V]/18)$  and SWE. They also suggested using 37H and 37H polarization differences for identifying wet snow. Derksen et al. (2004) developed a new algorithm which derives SWE for open environments, deciduous, coniferous, and spars forest cover  $[SWE = F_D SWE_D + F_C SWE_C + F_S SWE_S + F_O SWE_O]$ . The algorithm represents an improvement, however

---

<sup>1</sup> NOAA-CREST, City University of NY, 137thst & Convent Ave. New York, NY.

still underestimates SWE in densely forested areas. Tedesco et al. (2004) developed and tested an inversion technique for retrieval of SWE and dry snow depths based on artificial neural networks (ANN) by using 19- and 37-GHz SSM/I measured brightness temperatures.

Hallikainen et al 2003 combined active (QuikSCAT/SeaWinds) and passive (SSMI/DMSP) data for monitoring key snow parameters in Finland. The results show that combined active and passive microwave sensors provide useful diurnal and seasonal information. These results are more accurate than those obtained by only passive microwave. In another research Hallikainen showed that using space borne scatterometer (QuikSCAT onboard SeaWinds) for dry snow conditions, the backscattering coefficient increases with increasing SWE. For wet snow condition backscattering coefficient decreases with increasing SWE. Ku-band scatterometer were used successfully to determine the onset and the end of snow melt, and to derive time series for the fraction of snow-free ground during the seasonal snow melt period (Hallikainen et al 2004).

Synthetic Aperture Radar (SAR) particularly C-band SAR has shown the potential for monitoring snow and ice for more than two decades. The high spatial resolution and the independence of the sensors from sun illumination and cloud cover make SAR an ideal tool for snow studies. Launched in 1995, Radarsat-1 offers spatial resolutions between 10m to 100m and a swath up to 500km. To estimate SWE using C-band SAR, Bernier et al. (1998) introduced an approach based on the fact that snow cover characteristics influence the underlying soil. The snow influence on soil temperature affects the dielectric properties of the soil which has a major role on the backscattered signal. To recover the SWE from SAR data an algorithm made of two equations was used. The first equation defines a linear relationship between the snow thermal resistance and the backscattering ratio between a winter image and a reference (snow-free) image in DB. The snow-free image helps to eliminate the radiometric distortion due to topography as well as to minimize the effect of soil roughness on the signal. The second equation is a linear relationship between thermal resistance and the SWE. To estimate SWE from thermal resistance the mean density of the snowpack has to be derived. This approach has been applied for cold winter conditions and dry snow (Bernier et al. 1999). The critical variables influencing the algorithm are variety of land cover, specifically forest density, Snowpack properties (depth>2m), and severe topography. In a research on passive and active airborne microwave remote sensing of snow cover Sokol et al. (2003) showed that SAR sensors are highly sensitive to changes in the dielectric constant and have better spatial resolution than their passive counterparts. They concluded that passive techniques estimate SWE most accurately under dry snow conditions with minimal stratified snow structures (Sokol et al. 2003).

The focus of this research is estimating Snow Water Equivalent (SWE) in Great Lakes area by using active and passive microwaves. Different approaches were examined for SWE estimations by RADARSAT SAR and also QuikSCAT-Ku along and passive SSM/I.

## **STUDY AREA**

It is also located on the transitional zone for snow meaning that the northern part of the study area is covered by snow for the whole winter season however for the southern part there is a pattern of snow-fall and snow melt within the season. In addition to snow pattern, the land cover type varies a wide range including, Evergreen Needle leaf forest, Deciduous Broadleaf forest, cropland, woodland and dry land (Figure 1).

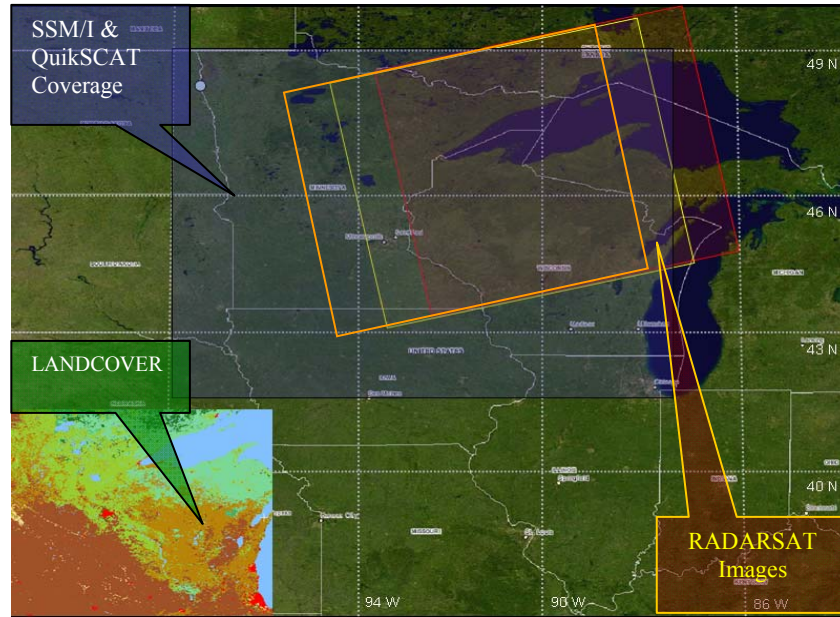


Figure 1. Study area and SSM/I and RADARSAT coverage

## DATA USED

### SSM/I

SSM/I passive microwave radiometer with seven channels is operating at five frequencies (19, 35, 22, 37, and 85.5 GHz) and dual-polarization (except at 22 GHz which is V-polarization only). The sensor's spatial resolution varies for different channel frequencies. In this study we used Scalable Equal Area Earth Grid EASE-Grid SSM/I products distributed by National Snow and Ice Data Center (NSIDC). EASE-Grid spatial resolution is slightly more than 25km (25.06) for all the channels (NSIDC) although the recorded resolution of the sensor for longer wavelengths is more than 50km. The three EASE-Grid projections comprise two azimuthal equal-area projections for the Northern or Southern hemispheres, respectively and a global cylindrical equal area projection. In our study we used a Northern hemisphere azimuthal equal-area. The study area is covered by 980 (28 by 35) SSM/I EASE-Grid pixels.

### Ku-Band

The QuikSCAT/SeaWinds scatterometer provides normalized radar cross section measurements of the Earth's surface at unprecedented coverage and resolution. The QuikSCAT sensor on the SeaWinds satellite operates at 13.4 GHz vertical and horizontal channels. The sigma (0) browse product of QuikSCAT has the grid size of 5 pixels per degree or about 22.5km at the equator. In order to match SSM/I grid size the QuikSCAT images were averaged to 25km resolution for the study area.

### Normalized Difference Vegetation Index (NDVI)

NDVI is used to represent the variety of land cover in the study area. The NDVI data obtained from the NOAA/NASA Pathfinder AVHRR is distributed at Goddard Space Flight Center (GSFC). The spatial resolution is 8km by 8km obtained within a 10 day period that has the fewest cloud. To match the with RADARSAT images, NDVI image was resampled and projected to UTM.

### **RADARSAT Images**

RADARSAT ScanSAR images were obtained for February 06, 2003 (winter image), February 02, 2006, and May 01, 2002 (snow-free image) as show in Table 1. ScanSAR images (500km by 500km) have the nominal spatial resolution of 100m. The ScanSAR products currently offered by us do not come in a map-projected format. However, images have the geo-referencing information contained in the CEOS format. This information is derived from the satellite orbit (ephemeris) and is typically accurate to 100–200 meters, depending on beam mode and the topography. To reduce geometric distortions caused by radar sensor viewing geometry satellite movement, earth curvature and rotation, both RADARSAT images were registered to a Landsat image of the study area. More than 15 Ground Control Points and a second order model and nearest neighbor resampling mode were used to register the RADARSAT images. The images were projected to a UTM projection and subseted for the in-common area of coverage.

**Table 1. RADARSAT images for Great Lake area**

Image	Date	Time(UTC)	Inc Angle	NW	NE	SW	SE	Center
Winter	2/2/2006	23:47	34.26	48 51 N 94 13 W	49 46 N 86 37 W	43 43 N 92 27 W	44 37 N 85 33 W	46 44 N 89 42 W
Winter	2/6/2004	23:53	34.26	48 26 N 94 47 W	49 17 N 87 46 W	43 50 N 93 17 W	44 40 N 86 50 W	46 53 N 90 44 W
Snow-free	5/1/2003	23:49	34.26	48 37N 93 47 W	49 27 N 86 45 W	44 00 N 92 17 W	44 51 N 85 49 W	46 47 N 89 40 W

### **Ground Truth Data**

NOAA National Weather Service's National Operational Hydrologic Remote Sensing Center (NOHRSC) started producing SNOW Data Assimilation System (SNODAS), beginning 1 October 2003. SNODAS includes and procedures to assimilate airborne gamma radiation and ground-based observations of snow covered area and snow water equivalent, downscaled output from Numerical Weather Prediction (NWP) models combined in a physically based, spatially distributed energy- and mass-balance model. The output product has 1km spatial and hourly temporal resolution.

### **METHODOLOGY AND MODEL**

The objective of this study is to estimate snow depth and SWE using active and passive microwave images. However, active microwave RADARSAT SAR and passive microwave SSM/I are totally different in their nature and applications. RADARSAT images have high spatial resolution and are suitable for regional studies. On the other hand, low spatial resolution and high temporal resolution of SSM/I make it suitable for studies on a global scale. In order to consider above differences, each of the active and passive data were analyzed separately to investigate their potential to estimate snow parameters. This section focuses on: 1) Using high resolution active microwave RADARSAT SAR to estimate SWE. This section focuses on how to process RADARSAT images and corresponding ground truth data along with suggesting modeling approaches to improve the estimations. 2) Using low resolution passive SSM/I and active QuikSCAT with statistical based models. Also, the improvement by combining various data types was quantified.

An adaptive network is a network structure that consists of a number of nodes (neurons) connected through directional links. Each node represents a process unit, and the links specify casual relationship between the connected nodes. Nodes are adaptive meaning that the outputs of these nodes depend on modifiable parameters pertaining to these nodes. The learning rule specifies how these parameters should be updated to minimize error which is discrepancy between the networks actual output and desired one. In our study we used a feed forward backpropagation

model. The network has two hidden layers with ten nodes at each layer. To train the network data were divided into three sets (training, validation, and test). The model testing is the process by which the input vectors from input/output data sets on which the network is not trained, are presented to the trained model, to see how well the ANN model predicts the corresponding data set output values. The other type of validation which is also referred as checking data set is used to control the potential for the model over fitting the data. In principle, the model error for the checking data set tends to decrease as the training takes place up to the point that overfitting begins, and then the model error for checking data suddenly increases.

### High Resolution Active Microwave RADARSAT SAR

Four different approaches for ANN input data were considered: A. Input consists of the only backscattering ration at 25km resolution. B. Input includes NDVI data in addition to backscattering both in 25km resolution. C. Input includes NDVI data in addition to backscattering with modified ANN training. D. Input includes NDVI and Backscattering in 5km averaged resolution.

#### *A. Input consists of the only backscattering ration at 1km resolution*

In the first approach, the backscattering ratio was used as the input for the ANN model. Figure 5.8 shows the spatial variation of the backscattering ratio while the water bodies are filtered out of the image. The higher backscattering ratio is detected in high latitudes and around the lake. The scatter plot of backscattering versus the SWE indicates low correlation.

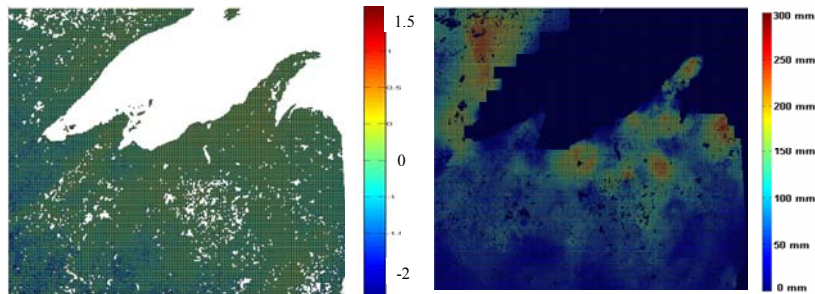


Figure 2. Spatial variation of backscattering ratio and SWE in 1km resolution, February 06, 04

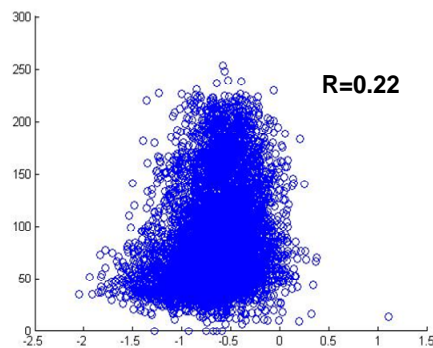


Figure 3. Backscattering vs. SWE, February 06, 04

The ANN model was trained using backscattering ratio as input and SWE the output of the model. The simulated SWE based on the backscattering ratio for February 06, 2004 is shown in Figure 4. Both the produced image and the corresponding scatter plot show unsatisfactory results. The model output is highly underestimated and show very low correlation coefficient. Introducing land cover characteristics can be helpful to increase the accuracy of the model.

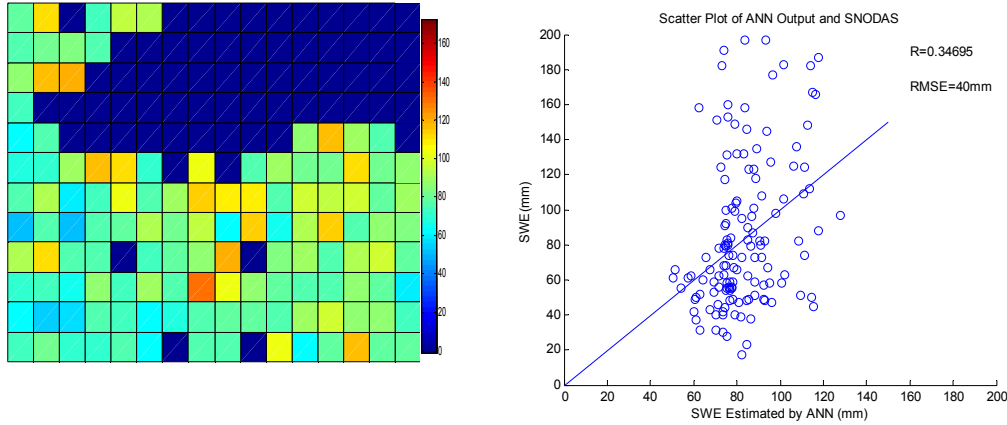


Figure 4. Spatial variation of SWE for February 06, 04 and the scatter plot of model output vs. ground truth SWE

*B. Input includes NDVI data in addition to backscattering both in 1km resolution*

In order to introduce the land cover characteristics in a quantitative way the NDVI image of the study area was added as an input to the ANN model. The model was trained and validated using the data from two winter days of February 06, 2004 and February 02, 2006. The simulated SWE for February 06, 2004 is illustrated (Fig 5).

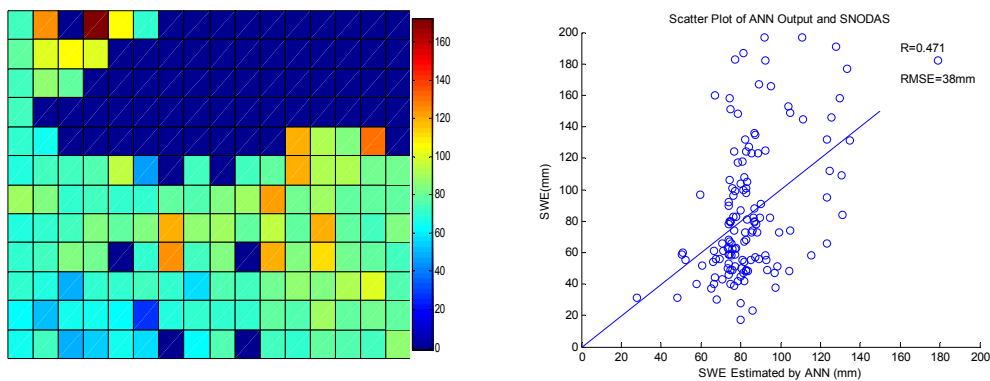


Figure 5. Simulated SWE based on NDVI and Backscattering for February 06, 04 and the scatter plot of model output vs. ground truth SWE

The above results show the increase of correlation by adding the NDVI to the ANN model. On the other hand, the problem with underestimation of SWE still exists. As shown in the scatter plot, for SWE varying between 0 to 250mm the model output mostly varies between 50 to 150mm. This problem might originate from the training process considering the fact that there are more pixels with low values of snow than high values. This forces the training towards the low values in order to minimize the RMSE of the total estimation. To minimize the influence of number of the pixels with different values for SWE, the network was trained with same number of pixels from each class as the third approach.

*C. Input includes NDVI data in addition to backscattering with modified ANN training*

In the third approach the pixels were divided to four classes based on the SWE values ( $SWE < 50$ ,  $50 < SWE < 75$ ,  $75 < SWE < 175$ ,  $SWE > 175$ mm). A fixed number of pixels from each class were selected for training the ANN. The neural network was trained and simulated. Figure 6 shows the spatial variation of the simulated SWE.

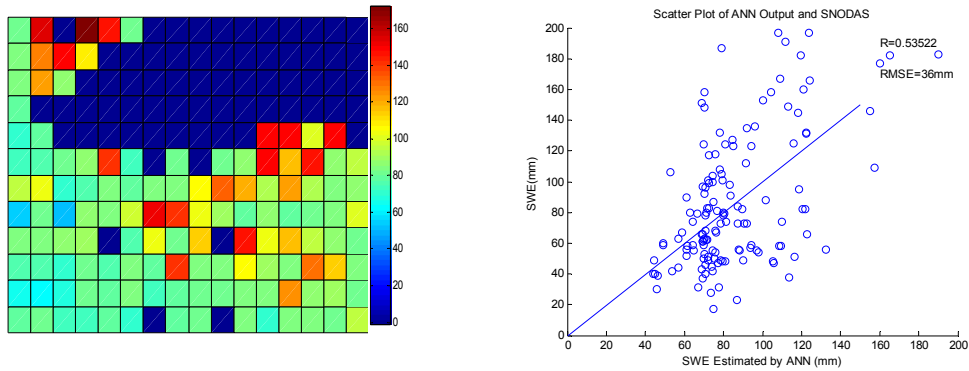


Figure 6. Simulated SWE based on NDVI and Backscattering using equal number of pixels from each class

The above results confirm the effect of classification in the training process. The scatter plot shows an increase in the range of estimated SWE from 120 to 175mm.

*D. Input includes NDVI and Backscattering in 5km averaged resolution.*

The final approach consists of decreasing the resolution to 5km. Both the backscattering image and the ground truth data were averaged to 5km resolution using the nearest neighbor method for resampling (Fig 7).

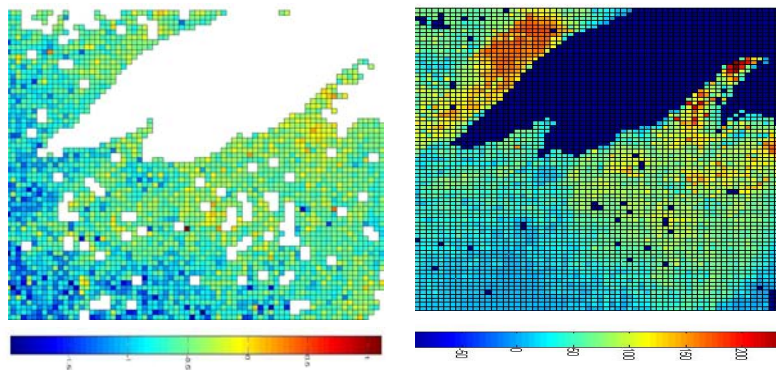


Figure 7. Backscattering ratio (left) and SWE (right) for Feb. 06, 04 averaged to 5km X 5km

Figure 8 shows the variation of backscattering ratio and SWE for all pixels in the study area. First pixel is located in the lower left corner of the images. The variation of SWE has a consistent trend. It increases by number of the pixels which indicates higher SWE in the northern part of the

image. On the other hand, the backscattering ratio trend is almost constant. Also, the range for the ratio is highly different for years 2004 and 2006. This limits any kind of modeling for estimating SWE from backscattering. The comparison of the scatter plots of SWE versus backscattering is shown in Figure 9.

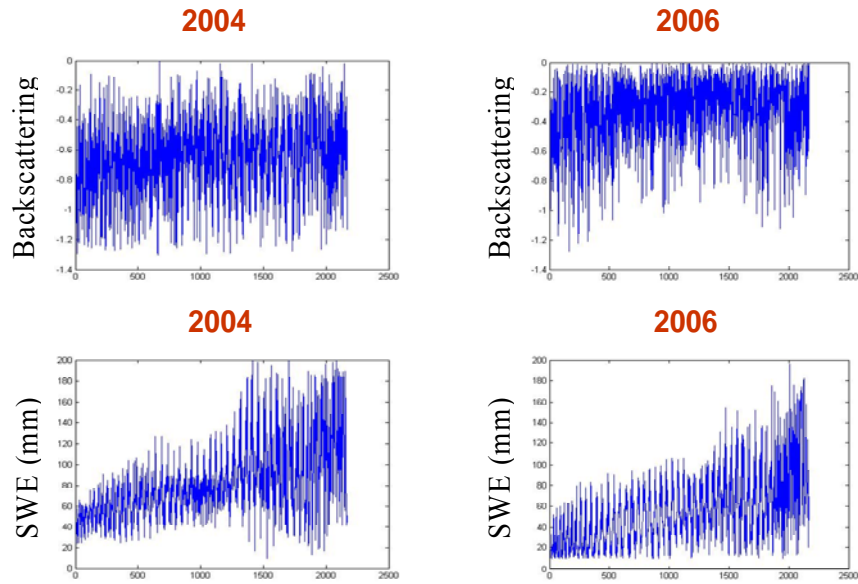


Figure 8. Variation of backscattering ratio and SWE for different parts of the study area

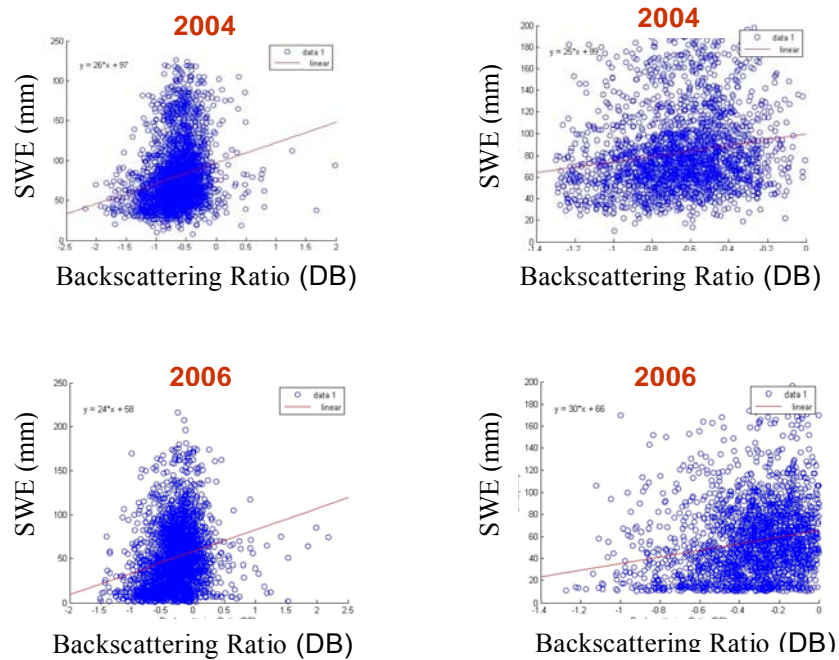


Figure 9. Scatter plots of Backscattering vs. SWE at 5km resolution for two images (Feb 06, 04 & Feb 02, 06)



The left scatter plots representing the complete dataset and the right ones are modified by eliminating the backscattering ratio higher than zero since only few percentage points are points have backscattering values higher than zero. This could be the effect urban areas that have high backscattering. The new scatter plots are shown in Figure 9. These scatter plots clearly show where SWE is in the range of 10mm to 60mm the backscattering range is very large. Also, the backscattering range between two years (2004 and 2006) is very different. This indicates that developing a model to estimate SWE using backscattering ratio is very difficult. A solution for this problem is modifying the model for each year.

### Low Resolution Active QuikSCAT and Passive SSM/I

#### A. Evaluation of using NDVI and QuikSCAT in SWE estimation

A feed forward backpropagation neural network model with 2 hidden layers, 20 neurons each layer, was developed. The output of the model consists of ground truth SWE data from NOHRSC. In order to evaluate the effect SWE on various microwave channels different combination of inputs were used. First, the input consisted four of SSM/I channels (19V, 19H, 37V, and 37H). Then, NDVI and SSM/I were introduced as the input to the model. Finally, QuikSCAT-ku along with SSM/I and NDVI were used as the input. For all above approaches the model was validated by a dependent data. In other words, the training and validation data were the same. Figure 10 shows the results for various approaches. SSM/I brightness temperatures have shown correlations with SWE to some extent. Adding NDVI to the input brings information about the land cover type for the ANN model and increases the accuracy of the estimate. By adding active QuikSCAT to the input we have an input of three independent data sets. The increase of correlation coefficients indicates that combining active and passive using a neural network can improve the SWE estimation. Figure 10 also indicates that combining SSM/I with QuikSCAT and NDVI produces the best results. The sudden decrease of correlation coefficients for days in February should be due to the existence of wet snow in parts of the study area which was already explained in chapter for snow cover estimation.

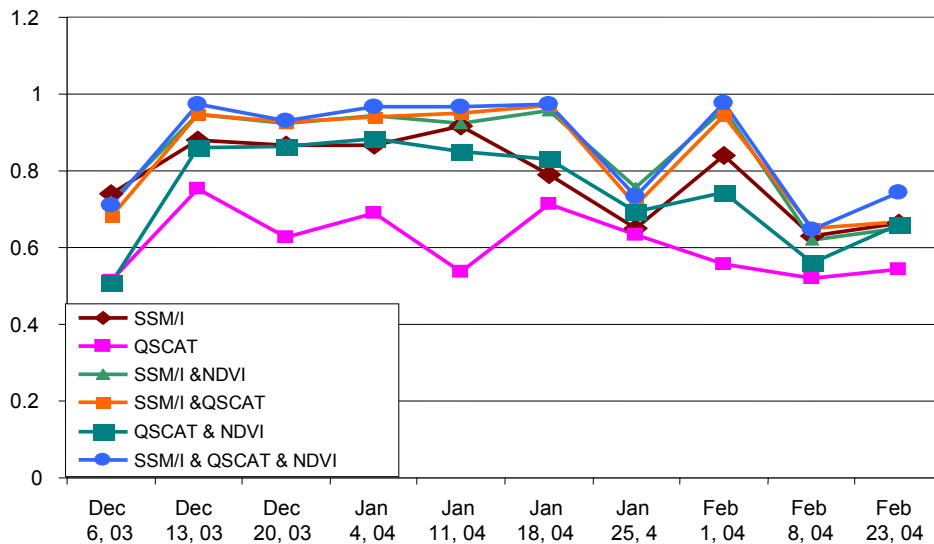


Figure 10. Correlation coefficients ( $R^2$ ) between estimated SWE and the corresponding ground truth data (winter 2003–2004, model validated by dependent data)

*B. Using Active and Passive to Estimate SWE*

The results above showed that adding NDVI and QuikSCAT-ku increases the correlation between input of microwave channels and SWE. To investigate the capability of the model to estimate SWE, it was examined to independent data. The approach consisted of training the model with the data from the days before the selected day for estimation. Table 2 describes the approach. The results for correlation coefficients and RMSE in the table show an increasing trend for RMSE. This increase in the error originates from the increase in the average depth of snow during the winter season. For correlation coefficients there is an improvement in the beginning but it decreases after January 25, 2004. For the selected days in February especially Feb08, Feb16, and Feb23, The error increases dramatically. This is due to the wet snow conditions for those days. Wet snow can not be detected by passive SSM/I scattering channels. This section is already discussed in snow cover section. Figures 11 and 12 show the estimated snow for February 01, 2004. It is observed that the model is incapable of detect and estimating deep snow. The scatter plot of the ground truth versus the estimate (Fig 11) illustrates the results in a quantitative way. The best fitted line (red line) is below the 1:1 line indicating underestimation of the estimate.

**Table 2: Estimating SWE by ANN model**

<b>Training Data (Days)</b>	<b>Validation Data (Day)</b>	<b>Correlation Coe.</b>	<b>RMSE</b>	<b>Bias</b>
Dec06,Dec13	Dec 20	0.37	21	-14
Dec06, Dec13,Dec20	Jan04	0.43	17	1
Dec06,Dec13, Dec20, Jan04	Jan11	0.47	19	5
Dec13,Dec20, Jan04,Jan11	Jan18	0.44	30	-11
Dec20,Jan04, Jan11,Jan18	Jan25	0.53	45	-34
Jan04,Jan11, Jan18,Jan25	Feb01	0.47	44	-30
Jan18,Jan25, Feb01	Feb08	0.37	42	-31
Jan18,Jan25 Feb01,Feb08	Feb16	0.12	75	-58
Jan25, Feb01, Feb08, Feb16	Feb23	0	90	-83

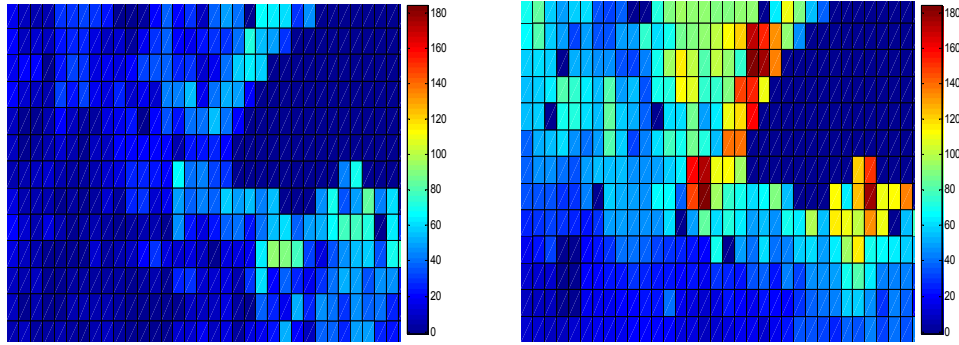


Figure 11. Estimated SWE by ANN (left) and SNODAS ground truth SWE (right), February 01, 2004

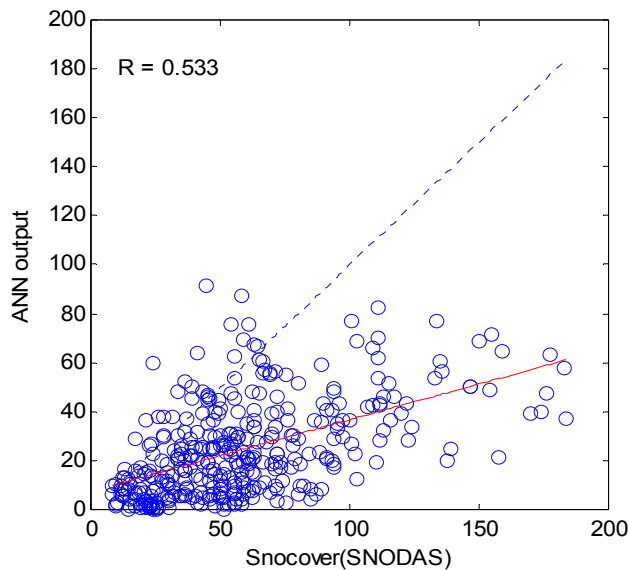


Figure 12. Estimated SWE by ANN vs. SNODAS ground truth SWE, February 01, 2004

## CONCLUSION

Three RADARSAT images were obtained to investigate the potential of RADARSAT SAR in estimating SWE. The images were processed and georeferenced using PCIGeomatica. The Ground truth data were obtained from NOHRSC SNODAS dataset through NSIDC. The backscattering ratio of RADARSAT images was derived by subtracting them from a reference image. The analysis indicates that backscattering ratio has limited correlation with SWE (20 percent). An ANN model was used to explore non-linear relationships between backscattering ratio and SWE. The results showed low correlation between estimated and ground truth SWE. In order to introduce land cover characteristics, an NDVI image was added to the input of the ANN model. The results showed a more than 15 percent improvement in correlation coefficient. To improve the estimation the input classified based on SWE values. This improved the range of the estimated SWE although it did not change the correlation coefficients. Finally the resolution was changed to 5km. It was concluded that where SWE is in the range of 10mm to 60mm the backscattering range is very large. Also, the backscattering range between two years (2004 and 2006) is very different. This indicates that developing a model to estimate SWE using backscattering ratio is very difficult. A solution for this problem is modifying the model for each year.

In case of low resolution passive SSM/I and active QuikSCAT, the ANN model shows satisfactory result in dependent estimation of SWE. Also, adding QuikSCAT-Ku increased the accuracy of the estimated SWE by neural networks. It was concluded that estimating SWE by neural networks is highly dependent on training data. This can become a source of error on model development. In order to resolve this problem a large dataset is necessary.

#### ACKNOWLEDGEMENTS

The Authors express their gratitude to Dr Jeff Hurley, a Senior Project Manager in RADARSAT International, for his support in processing and analyzing RADARSAT images.

#### REFERENCES

- Bernier M, Fortin J (1998). The Potential of Time Series of C-Band SAR Data to Monitor Dry and Shallow Snow Cover. *IEEE Transaction on Geoscience and remote sensing*, **36(1)**: 226–242.
- Bernier M, Fortin J Y, Gauthier, R, Gauthier, R, Roy, and P. Vincent (1999i). Determination of Snow Water Equivalent using RADARSAT SAR data in eastern Canada. *Hydrological Processes*, **13**:3041–3051.
- Chang, A. T. C, L. Foster, D. K. Hall. (1987). Nimbus-7 SMMR derived global snow cover parameters. *Annals Glaciology*, **9**:39–44.
- Derksen, E. LeDrew, A. Walker, and B. Goodison (2001). Evaluation of a Multi-Algorithm Approach to Passive Microwave Monitoring of Central North American Snow Water Equivalent. *IEEE*, 952–954.
- Hallikainen, M. T. (1984). Retrieval of snow water equivalent from Nimbus-7 SSMR data: effect of land cover categories and weather conditions. *IEEE Oceanic Engineering*, **9(5)**: 372–376.
- Hallikainen, M. T, P. Halme, M. Takala, J. Pulliainen (2003). Combined Active and Passive Microwave Remote Sensing of Snow in Finland. *IEEE*:830–832.
- Hallikainen, M. T, P. Halme, P. Lahtinen, M. Takala, J. Pulliainen (2004). Retrieval of Snow Characteristics from Scapeborne Scatterometer Data. *IEEE*:1849–1852.
- Sokol, J, T. J. Pultz, and A. E. Walker (2003). Passive and Active microwave remote sensing of snow cover. *INT. J. Remote Sensing*, **24(24)**:5327–5344.
- Tedesco, J. Pulliainen, M. Takala, M. Hallikainen, P. Pampaloni. (2004). Artificial neural network-based techniques for the retrieval of SWE and snow depth from SSM/I data. *Remote Sensing of Environment* **90**:76–85.
- Walker, G. B. E. a. A. E. (1995). Canadian development and use of snow cover information from passive microwave satellite data. *Passive microwave remote sensing of land-atmosphere interactions*. B. J. Choudhury, Y. H. Kerr, E. G. Njoku and P. Pampaloni. The Netherlands, VSP BV 245–262.